ELSEVIER

Biophysical Chemistry xx (2003) xxx–xxx

Biophysical Chemistry

www.elsevier.com/locate/bpc

Rational modelling of the voltage-dependent K^+ channel inactivation by aminopyridines

Alfonso Niño[a,*], Camelia Muñoz-Caro[a], Ramón Carbó-Dorca[b], Xavier Gironés[b]

[a]*Grupo de Química Computacional, Escuela Superior de Informática, Universidad de Castilla-La Mancha, Paseo de la Universidad 4, 13071 Ciudad Real, Spain*

[b]*Institute of Computational Chemistry, University of Girona, Campus Montilivi, 17071 Girona, Catalonia, Spain*

Received 14 October 2002; received in revised form 22 January 2003; accepted 22 January 2003

Abstract

A functional model for the in vitro inactivation of voltage-dependent K^+ channels is developed. The model expresses the activity as a function of the aminopyridine pK_a, the interaction energy with the receptor, and a quotient of partition functions. Molecular quantum similarity theory is introduced in the model to express the activity as a function of the principal components of the similarity matrix for a series of agonists. To validate the model, a set of five active (protonated) aminopyridines is considered: 2-aminopyridine, 3-aminopyridine, 4-aminoquinoleine, 4-aminopyridine, and 3,4-diaminopyridine. A regression analysis of the model gives good results for the variation of the observed activity with the overlap similarity index when pyridinic rings are superposed. The results support the validity of the model, and the hypothesis of a ligand–receptor entropy variation depending mainly on the nature of the ligand. In addition, the results suggest that the pyridinic ring must play an active role in the interaction with the receptor site. This interaction with the protonated pyridinic nitrogen can involve a cation–π interaction or a donor hydrogen bond. The amine groups, at different relative positions of the pyridinic nitrogen, can form one or more hydrogen bonds due to the C_4 symmetry of the inner part of the pore in the K^+ channel.

Keywords: K^+ channel blocking; Aminopyridines; Activity model; Molecular quantum similarity

1. Introduction

Aminopyridines are bioactive N-heterocyclic tertiary amines, which block the voltage-dependent K^+ channels [1–3]. In this form, the efflux of intracellular K^+ is suppressed, and the pre-synaptic action potential is maintained. The result is an increase of the nerve signal [2]. Due to this capacity of enhancing nerve transmission, aminopyridines have been applied to reverse anaesthesia and muscle relaxation [3]. In addition, they have been proposed and tested as drugs for the treatment of myasthenia gravis [4], multiple sclerosis [5], spinal cord injuries [6], and botulism [7]. Also, aminopyridines have been tested as putative agents for the symptomatic treatment of Alzheimer's disease [8]. In particular, 4-aminopiridyne, under the name fampridine, is now being used in large-scale human trials as an agent for compensating the loss of the myelin cover in damaged nerves [9].

*Corresponding author. Tel.: +34-926-2953-62; fax: +34-926-2953-54.

E-mail address: quimcom@uclm.es (A. Niño).

0301-4622/03/$ - see front matter © 2003 Published by Elsevier Science B.V.
doi:10.1016/S0301-4622(03)00030-9

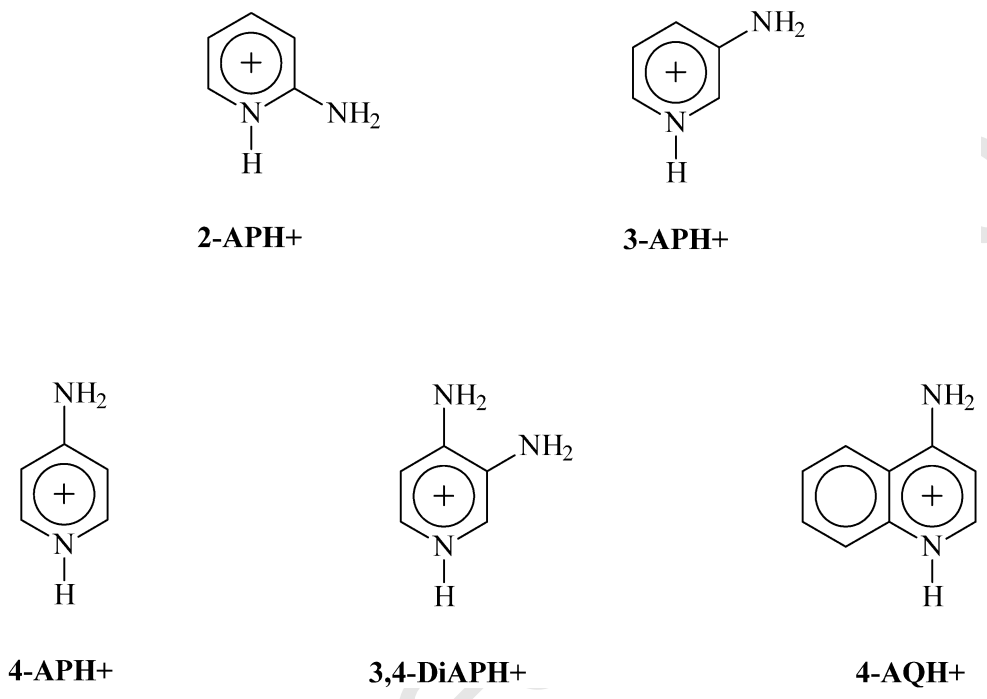

Fig. 1. Structure of the protonated aminopyridines considered in this work.

Aminopyridines are weak basis, with pK_a value in the range 6–9. Thus, they can exist in neutral and protonated forms at physiological pH. The experimental [10–15] and theoretical evidence [16,17], identify the protonated form as the active species for the inactivation of K^+ channels. In addition, all these studies established an intracellular and reversible way of action. These works also identify the pharmacophore of aminopyridines as constituted by the positive charge on the protonated ring, and one or more amine groups suitable for hydrogen bonding. The theoretical studies show that protonation is essential for the different aminopyridines to get a topologically similar electron density distribution. Recently, new additional theoretical work has been carried out on both the role played by the positive charge in the interaction with the receptor site, and on the 3-D structure of the K^+ channel [18]. These studies have shown that the electrostatic interaction with acidic groups is not compatible with the observed activity variation, in contrast with previous proposals [16]. Despite these studies, the nature of the receptor site is not still determined. At present, the most plausible hypothesis is that the receptor site is defined by a fourfold structure, C_4 symmetry, of hydrogen donor/acceptor amino acid residues placed in the K^+ channel pore [18]. The role played in the inactivation of the K^+ channel by the specific characteristics of aminopyridines (pK_a, affinity for the receptor, electron density distribution) is not yet established.

In this work, we develop a physical–mathematical model of activity for K^+ channel blocking by aminopyridines. Thus, we consider the experimental conditions used for determining the available, in vitro, activity data for a series of active (protonated) aminopyridines: 2-aminopyridine (2-APH$^+$), 3-aminopyridine (3-APH$^+$), 4-aminoquinoleine (4-AQH$^+$), 4-aminopyridine (4-APH$^+$), and 3,4-diaminopyridine (3,4-DiAPH$^+$), see Fig. 1. The model accounts for the intra and extracellular protonation equilibria, and for the reversible interaction with the receptor site. In addition, we apply the molecular quantum similarity theory [19] to express the activity vari-

ation as a function of the principal components of quantum similarity matrices. We contrast the resulting model, and its inner assumptions, against the observed activity data. Thus, we use different similarity indices and different molecular orientations of the aminopyridines. The role played by different molecular interactions in the binding to the receptor is also considered.

2. Theory

The available in vitro experimental activity index for the considered set of aminopyridines, see Fig. 1, corresponds to the concentration, c, that increases five times the mean quantal content of end-plate potentials at the frog neuromuscular junction [13]. Activity data were measured on isolated sciatic nerve sartorius muscle preparations, within a high magnesium–low calcium Ringer solution in a bath at a temperature of 20 °C [13].

To develop the activity model, we consider a nerve cell surrounded by an extracellular medium, the whole system being at equilibrium. Due to the pK_a range of aminopyridines, in the extracellular medium we can find the protonated and neutral forms. However, only the neutral form can cross the lipidic cell membrane, passing to the intracellular medium. Here, the system will protonate again to yield the active, charged form. Finally, the active form interacts reversibly with the receptor site. All these steps are shown in Fig. 2.

Following the previous description, the neutral aminopyridine, AP, will protonate in solution, leading to the charged form, APH^+, according to the equilibrium,

$$APH^+ + H_2O \rightleftharpoons AP + H_3O^+ \qquad (1)$$

with acidic constant K_a. Thus, at equilibrium we have in the extracellular medium an AP concentration,

$$|AP|_e = K_a \frac{|APH^+|_e}{|H_3O^+|_e} \qquad (2)$$

where the subscript e stands for extracellular. A similar relation holds for the intracellular medium.

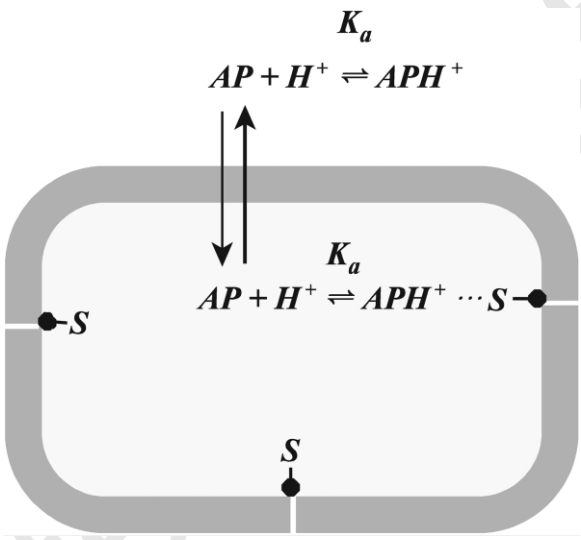

Fig. 2. Schematic representation of the different phenomena involved in the interaction between aminopyridines and its intracellular receptor site in the K^+ channel of nervous cells. In the draw, S represents the active site.

Considering the permeability of the lipidic cell membrane to the neutral form, and the equilibrium condition, we have,

$$|AP|_e = K_a \frac{|APH^+|_i}{|H_3O^+|_i} \qquad (3)$$

where the subscript i stands for intracellular, and $|AP|_e$ is the experimental activity index, c.

Taking into account the reversible interaction of the active, protonated, form of aminopyridines with the receptor site we will have at equilibrium,

$$K = \frac{|S\cdots APH^+|}{|S||APH^+|_i} \qquad (4)$$

where K represents the aminopyridine-active site binding constant, $|S|$ is the concentration of active sites, and $|S\cdots APH^+|$ is the concentration of aminopyridine-active site complexes. From Eqs. (3) and (4), and the pK_a definition we get,

$$\log c = \log\left(\frac{|S\cdots APH^+|}{|S|\,|H_3O^+|_i}\right) - pK_a - \log K \qquad (5)$$

Since we have a series of structurally-related compounds sharing the same action mechanism, and since the intracellular pH can be considered constant, we can assume that along the series,

$$\Delta\log\left(\frac{|S\cdots \mathrm{APH}^+|}{|S|\,|\mathrm{H_3O}^+|_i}\right) \ll \Delta(-\mathrm{p}K_a - \log K) \qquad (6)$$

As long as Eq. (6) holds, Eq. (5) shows that the activity variation is two-dimensional, depending on the acidic constant and the Gibbs energy variation for the interaction with the receptor. Eq. (5) explains the observation by Molgó et al. [13] about the lack of a direct dependence of the activity on the pK_a.

Since for our considered series of aminopyridines the pK_a values are known in Molgó et al. [20], we can focus in the last term of Eq. (5), log$K$. The K constant can be thermostatically determined from the microscopic (quantum) description of the system [21]. Thus,

$$K = \frac{Q_{S\cdots \mathrm{APH}^+}}{Q_S Q_{\mathrm{APH}^+}} \exp\left[-\Delta E/kT\right] \qquad (7)$$

where the Qs are canonical partition functions and $\Delta E = E_{S\cdots \mathrm{APH}^+} - E_S - E_{\mathrm{APH}^+}$.

Using Eqs. (5) and (7) we obtain,

$$\log c = \log\left(\frac{|S\cdots \mathrm{APH}^+|}{|S|\,|\mathrm{H_3O}^+|_i}\right) - \mathrm{p}K_a + \log\left(\frac{Q_S Q_{\mathrm{APH}^+}}{Q_{S\cdots \mathrm{APH}^+}}\right) + 0.43429\frac{\Delta E}{kT} \qquad (8)$$

There is a huge difference in the number of intramolecular degrees of freedom between a macromolecular receptor and usual bioactive ligands. In addition, considering a series of compounds sharing a common action mechanism, the initial structure of the receptor is the same for all the compounds. In turn, we have also found that the final structure of the complex with the receptor is very similar for all these compounds. Taking into account the previous points, the variation of the quotient of partition functions in Eq. (8) along the series, must depend mainly on the nature of the ligand. Since this quotient represents an entropic contribution, we have $\Delta\Delta S \simeq f(\mathrm{APH}^+)$ along the series. Therefore, Eq. (8) can be rewritten as,

$$\log c = \mathrm{A}(\mathrm{pH}_i,\, T) - \mathrm{p}K_a + B(\mathrm{APH}^+) \qquad (9)$$

where A is a constant (for constant intracellular pH, and temperature, T), and B is given by,

$$B = \log\left(\frac{Q_S Q_{\mathrm{APH}^+}}{Q_{S\cdots \mathrm{APH}^+}}\right) + 0.43429\frac{\Delta E}{kT} \qquad (10)$$

Since B is a microscopic magnitude, it corresponds to a quantum mechanical observable. Therefore, it can be determined by using a given hermitian operator. That is, we can determine B as the expectation value of an appropriate operator acting on the wave function of the aminopyridine. To establish a connection with quantum similarity measures, we will use the electronic probability density function, $\boldsymbol{\rho}(\mathbf{r})$, rather than the wave function. Thus, according to theoretical statistics, we have that the expectation value of a non-differential operator is given by [19,22,23],

$$\boldsymbol{B}_{\mathrm{APH}^+} = \langle \boldsymbol{\omega}_{\boldsymbol{B}} \rangle_{\mathrm{APH}^+} = \int \boldsymbol{\Omega}_{\boldsymbol{B}}(\boldsymbol{r}) \boldsymbol{\rho}_{\mathrm{APH}^+}(\boldsymbol{r}) \mathrm{d}\boldsymbol{r} \qquad (11)$$

where $\boldsymbol{\Omega}_{\boldsymbol{B}}$ is the operator corresponding to B, and ρ_{APH^+} is the first order electronic density function for each protonated aminopyridine. An example of Eq. (11) is the evaluation of the electronic part of the electrostatic molecular potential carried out by Bonaccorsi et al. [24]. When the operator contains a differential part, Eq. (11) contains an additional term related to the kinetic energy [25]. For a series of structurally-related compounds, previous work suggests the variation of this last term on the series to be negligible [26]. Eq. (11) is closely related to the concept of molecular similarity.

Similarity between two molecules, A and B, can be defined in quantum mechanical terms as [19,23,27],

$$\mathbf{z}_{\mathrm{AB}} = \int\int \boldsymbol{\rho}_A(\boldsymbol{r}_1) \boldsymbol{\Omega}(\boldsymbol{r}_1, \boldsymbol{r}_2) \boldsymbol{\rho}_B(\boldsymbol{r}_2) \mathrm{d}\boldsymbol{r}_1 \mathrm{d}\boldsymbol{r}_2 \qquad (12)$$

where $\boldsymbol{\Omega}$ represents a positive definite operator, which is usually the Dirac delta function $\boldsymbol{\delta}(\boldsymbol{r}_1-\boldsymbol{r}_2)$, or the Coulomb operator, $|\boldsymbol{r}_1-\boldsymbol{r}_2|^{-1}$. These options define the overlap or Coulomb molecular quantum similarity measures, respectively. The overlap measure can be interpreted as a shape index of similarity, whereas the Coulomb measure represents specifically an electrostatic descriptor.

For a given set of n agonists, a symmetric similarity matrix, $\mathbf{Z}$, can be defined as $\mathbf{Z}=\{z_{ij}\}$, with i, and j ranging from 1 to n. Using the similarity matrix, $\mathbf{Z}$, for our set of aminopyridines Eq. (11) reads,

$$\boldsymbol{B}^{\boldsymbol{T}}=w^{T}\boldsymbol{Z} \tag{13}$$

where $\boldsymbol{w}$ is the matrix representation of the operator $\boldsymbol{\Omega}$, see Eq. (12), in the basis of the density functions for the set of agonists [19,23]. The T superscript indicates a transpose matrix. Eq. (13) is a particular case of the discrete representation of expectation values, which is the basis of quantum QSAR (Q^2SAR) [19,25].

Quantum similarity measures can be normalised to the open interval (0, 1] yielding the Carbó indices [19] defined as,

$$C_{ij}=z_{ij}/(z_{ij}z_{jj})^{1/2} \tag{14}$$

which can be interpreted as the cosine of the angle subtended by the density functions $\boldsymbol{\rho}_i$ and $\boldsymbol{\rho}_j$. Carbó indices represent a natural and general way to measure the closeness of two molecular objects. We will deduce here, a relationship between Eq. (9) and Carbó indices. Defining the self-similarity measure for the ith molecule of the set as z_{ii}, we can construct a self-similarity (diagonal) matrix $\mathbf{S}=\{z_{ij}\}$. Thus, in matrix form, Eq. (14) can be written as,

$$\boldsymbol{C}=\boldsymbol{S}^{-1/2}\boldsymbol{Z}\boldsymbol{S}^{-1/2} \tag{15}$$

Using the $\boldsymbol{S}^{-1/2}$ matrix, and Eq. (15), we can reformulate Eq. (13) as,

$$\boldsymbol{B}'^{\boldsymbol{T}}=\boldsymbol{w}'^{\boldsymbol{T}}\boldsymbol{C} \tag{16}$$

where $\boldsymbol{B}'^{\boldsymbol{T}}=\boldsymbol{B}^{\boldsymbol{T}}\boldsymbol{S}^{-1/2}$ and $\boldsymbol{w}'^{\boldsymbol{T}}=\boldsymbol{w}^{\boldsymbol{T}}\boldsymbol{S}^{1/2}$. Eq. (16) is formally identical to Eq. (13), but in terms of Carbó indices and a trivially transformed $\mathbf{E}$ matrix.

Now, we can integrate our quantum similarity results with the activity model of Eq. (9). Reorganising Eq. (9) we have,

$$y=\log c+\mathrm{p}K_a=A(\mathrm{pH}_i,\,T)+B \tag{17}$$

Using matrix notation for Eq. (17), and taking into account Eqs. (13) and (16) we arrive at,

$$\boldsymbol{Y}'=\boldsymbol{A}'+\boldsymbol{w}'^{\boldsymbol{T}}\boldsymbol{C} \tag{18}$$

with $\boldsymbol{Y}'=\boldsymbol{Y}\boldsymbol{S}^{-1/2}$, and $\boldsymbol{A}'=\boldsymbol{A}\boldsymbol{S}^{-1/2}$, where $\boldsymbol{S}$ is the self-similarity matrix.

Eq. (18) shows that, if the assumed approximations are valid, there must exist a linear relationship between the $\boldsymbol{Y}'$ data and the Carbó indices for the series of protonated (active) aminopyridines.

Any similarity matrix for a series of n compounds is an $n\times n$ matrix. However, this amount of information is not necessary fully independent. Several inner factors can be assumed to exist. To identify them, different statistical techniques of multivariate analysis can be applied, in particular principal component analysis [28].

Applying principal component analysis to our problem we reduce the size of the initial matrix $\mathbf{C}$ to the minimum needed to describe the problem significantly. Principal components analysis performed on the covariance matrix provides a (reduced) $\mathbf{P}$ matrix of new factors, related to the old $\mathbf{C}$ matrix by a linear transformation,

$$\boldsymbol{P}=\boldsymbol{V}\boldsymbol{C} \text{ or } \boldsymbol{C}=\boldsymbol{V}^{-1}\boldsymbol{P} \tag{19}$$

where $\boldsymbol{V}$ is the matrix of eigenvectors of the covariance matrix. From Eqs. (18) and (19) we obtain,

$$\boldsymbol{Y}'=\boldsymbol{A}'+\boldsymbol{w}'^{\boldsymbol{T}}\boldsymbol{V}^{-1}\boldsymbol{P} \tag{20}$$

which is formally identical to Eq. (18), and express a multilinear relationship between the principal components, $\boldsymbol{P}$, and the $\boldsymbol{Y}'$ elements. In other words, knowing $\boldsymbol{Y}'$ and $\boldsymbol{P}$, multilinear least squares

must provide a good regression line when the model used to obtain the $\boldsymbol{Y}'$ and $\boldsymbol{P}$ components properly describes the experimental behaviour. Eq. (20) can then be used to test the validity of the approximations made in the functional model, Eq. (8), and to test different models of interaction with the receptor site.

3. Methods

The first order density matrices for the set of considered aminopyridines, are derived from the fully optimised structures of the protonated forms in aqueous solution [17]. These structures were determined at the B3LYP/cc-pVDZ level using the Polarizable Continuum Model (PCM). However, in order to avoid the computational cost associated with the calculation of quantum similarity measures at the B3LYP/cc-pVDZ level, a simpler procedure, based on fitted densities, is adopted. The electronic density function is expressed as a linear combination of discrete atomic contributions. These contributions are expressed as a convex combination of 1s Gaussians, which fit in the best possible manner, the original ab initio densities. This procedure is known as the promolecular Atomic Shell Approximation [29], and provides similarity measures that are within a 2% error interval compared to those measures computed using true ab initio densities. Here, a fitting to the Hartree–Fock/6-311G level has been used. Also, since similarity measures depend on the relative position of the structures in space, the topo-geometrical superposition approach (TGSA) [30] has been applied to align the structures. This procedure superimposes the structures based on molecular coordinates and atomic numbers toward the maximal common substructure shared by the molecules. After alignment of the structures, we have determined the overlap and Coulomb indices [19]. Principal components analysis has been carried out by means of the STATA statistical package [31].

4. Results and discussion

To test our model of activity, Eq. (20), we need the $\mathbf{Y}'$ components and the similarity measures for the set of considered molecules, see Fig. 1. Computation of $\mathbf{Y}'$ implies the evaluation of the $y = \log c + \mathrm{p}K_a$ values, see Eq. (17). Table 1 collects the y data as a function of the activity c, and the $\mathrm{p}K_a$. Considering its definition, Eq. (5) shows that y represents a measure of the affinity for the receptor (K constant). Table 1 shows that this affinity follows the order 4-AQH^+ > 4-APH^+ > 2-APH^+ ≃ 3,4-$DiAPH^+$ > 3-APH^+. It can be seen that this order is different from the raw order of activity. It is interesting to compare this affinity variation with the determined variation of interaction energy of the pyridinic ring of aminopyridines respect to an ionic or cation–π interaction [18]. We find that the present order of affinity is incompatible with the results presented in Muñoz-Caro and Niño [18] for the ionic interaction with an acidic group. However, we observe some similarity with the interaction energy for a cation–π interaction, where the π-electronic group interacts with the aminopyridine through the additional proton in the pyridinic ring. In particular, for a solvated aminopyridine and a cation–π complex in vacuum, 4-AQH^+ has the highest interaction energy. This result agrees with the data in Table 1. In addition, it is compatible with the fact that protonated aminopyridines are solvated in the intracellular medium before entering the K^+ channel. Also, it is compatible with the hypothesis that near a receptor site the bioactive compounds are not solvated, as in the case of enzymes [32].

Table 1
Activity, c, $\mathrm{p}K_a$, and y ($\log c + \mathrm{p}K_a$) values for the considered series of aminopyridines; the aminopyridines are collected in order of increasing in vitro activity

	C (μM)[a]	$\mathrm{p}K_a$[b]	y
2 APH^+	91.2	6.86	2.82
3 APH^+	38.2	5.98	1.56
4 AQH^+	26.0	9.17	4.58
4 APH^+	3.2	9.17	3.67
3,4 $DiAPH^+$	0.5	9.08	2.78

[a] Data taken from Molgó et al. [13].
[b] Data from Molgó et al. [20].

The overlap and Coulomb similarity measures, as well as the corresponding Carbó indices, are determined for the charged aminopyridines in solu-

Table 2
Similarity matrices for protonated aminopyridines

	3 APH$^+$	3,4 DiAPH$^+$	2 APH$^+$	4 APH$^+$	4 AQH$^+$
3 APH$^+$	267.09 (1.000)	235.95 (0.807)	150.22 (0.562)	131.02 (0.491)	185.37 (0.570)
3,4 DiAPH$^+$	235.95 (0.807)	320.20 (1.000)	136.18 (0.466)	228.50 (0.781)	236.36 (0.664)
2 APH$^+$	150.22 (0.562)	136.18 (0.466)	267.08 (1.000)	146.13 (0.547)	156.77 (0.482)
4 APH$^+$	131.02 (0.491)	228.50 (0.781)	146.13 (0.547)	267.09 (1.000)	202.71 (0.624)
4 AQH$^+$	185.37 (0.570)	236.36 (0.664)	156.77 (0.482)	202.71 (0.624)	395.59 (1.000)

The table contains the overlap quantum similarity measures. In parentheses the corresponding Carbó indices. Data obtained after maximising the common molecular substructures.

Table 3
Similarity matrices for protonated aminopyridines

	3 APH$^+$	3,4 DiAPH$^+$	2 APH$^+$	4 APH$^+$	4 AQH$^+$
3 APH$^+$	856.01 (1.000)	931.67 (0.972)	802.97 (0.937)	799.36 (0.934)	1072.25 (0.926)
3,4 DiAPH$^+$	931.67 (0.973)	1070.50 (1.000)	875.61 (0.914)	930.27 (0.972)	1221.39 (0.943)
2 APH$^+$	802.97 (0.937)	875.61 (0.914)	857.86 (1.000)	799.33 (0.933)	1067.27 (0.921)
4 APH$^+$	799.36 (0.934)	930.27 (0.972)	799.33 (0.933)	855.99 (1.000)	1059.73 (0.915)
4 AQH$^+$	1072.25 (0.926)	1221.39 (0.943)	1067.27 (0.921)	1059.73 (0.915)	1566.64 (1.000)

The table contains the Coulomb quantum similarity measures. In parentheses the corresponding Carbó indices. Data obtained after maximising the common molecular substructures.

Table 4
Similarity matrices for protonated aminopyridines

	3 APH$^+$	3,4 DiAPH$^+$	2 APH$^+$	4 APH$^+$	4 AQH$^+$
3 APH$^+$	267.09 (1.000)	152.38 (0.521)	190.60 (0.714)	237.15 (0.888)	230.64 (0.710)
3,4 DiAPH$^+$	152.38 (0.521)	320.20 (1.000)	120.35 (0.412)	200.01 (0.684)	218.01 (0.613)
2 APH$^+$	190.60 (0.714)	120.35 (0.412)	267.08 (1.000)	178.44 (0.668)	212.44 (0.654)
4 APH$^+$	237.15 (0.888)	200.01 (0.684)	178.44 (0.668)	267.09 (1.000)	223.54 (0.688)
4 AQH$^+$	230.64 (0.710)	218.01 (0.613)	212.44 (0.654)	223.54 (0.688)	395.59 (1.000)

The table contains the overlap quantum similarity measures. In parentheses the corresponding Carbó indices. Data obtained after superposing the amine groups and minimising the separation of the nitrogen atoms.

Table 5
Similarity matrices for protonated aminopyridines

	3 APH$^+$	3,4 DiAPH$^+$	2 APH$^+$	4 APH$^+$	4 AQH$^+$
3 APH$^+$	856.01 (1.000)	895.25 (0.934)	826.96 (0.965)	833.05 (0.973)	1039.33 (0.897)
3,4 DiAPH$^+$	895.25 (0.935)	1070.50 (1.000)	883.01 (0.921)	905.16 (0.946)	1132.39 (0.874)
2 APH$^+$	826.96 (0.965)	883.01 (0.921)	857.86 (1.000)	824.46 (0.962)	1034.57 (0.892)
4 APH$^+$	833.05 (0.973)	905.16 (0.946)	824.46 (0.962)	855.99 (1.000)	1040.66 (0.899)
4 AQH$^+$	1039.33 (0.897)	1132.39 (0.874)	1034.57 (0.892)	1040.66 (0.899)	1566.64 (1.000)

The table contains the Coulomb quantum similarity measures. In parentheses the corresponding Carbó indices. Data obtained after superposing the amine groups and minimising the separation of the nitrogen atoms.

tion. Tables 2 and 3 collect the results after maximising the largest common molecular substructure for each couple of aminopyridines. In all these cases, the resulting structures exhibit a superposition of the aromatic rings, with the two pyridinic nitrogens one on the other. In addition, and

Table 6
$\mathbf{Y}'$ ($\mathbf{Y}\,\mathbf{S}^{-1/2}$) matrices for the overlap and Coulomb similarity measures

	$\mathbf{Y}'^{a}$	$\mathbf{Y}'^{b}$
3 APH^+	0.096	0.053
3,4 $DiAPH^+$	0.155	0.085
$2APH^+$	0.173	0.096
4 APH^+	0.225	0.126
4 AQH^+	0.231	0.116

[a] Overlap similarity measure.
[b] Coulomb similarity measure.

taking into account that the interaction with the receptor involves the amine groups, we have tested a different set of superposed structures. Here, we have superposed the amine groups, maintaining the separation between the two pyridinic nitrogens on the ring as small as possible. The results are collected in Tables 4 and 5. All these possibilities correspond to four different models defined by Eq. (20). The models with superposed pyridinic rings correspond to the assumption that interaction with the aromatic ring influences the affinity for the receptor. On the other hand, the models with superposed amine groups correspond to the assumption of an affinity for the receptor determined solely by the interaction with the amine groups. In turn, comparison of the results for the Coulomb and overlap indices can be useful to analyse the importance of the electrostatic component in the process of interaction with the receptor.

To validate the four previous models, the corresponding $\mathbf{Y}'$ matrices, see Eq. (18), must be computed. Considering that $\mathbf{Y}' = \mathbf{Y}\mathbf{S}^{-1/2}$, where $\mathbf{S}$ is the self-similarity matrix, only two $\mathbf{Y}'$ matrices do exist, one for the overlap, and one for the Coulomb indices. Thus, using the data in Tables 1–5 and the definition of $\mathbf{Y}'$ we obtain the results collected in Table 6.

Principal components analysis is applied to the similarity matrices of Carbó indices collected in Tables 2–5. Since only five data points are available, we try to reduce the number of principal components as much as possible. In this form, fewer parameters must be determined in the subsequent least squares procedure needed to obtain Eq. (20). Thus, we consider two cases. First, we retain enough principal components to account for at least 70% of the variance. Second, we retain enough principal components to account at least for 95% of the total variance. With the retained principal components, a multilinear least squares procedure is applied following Eq. (20). The results are collected in Table 7.

The results show that a maximum of three principal components is only needed to describe fully (in more than 97%) the original variance. This represents a reduction in two of the five original similarity vectors, one for each aminopyridine, collected in Tables 2–5. Table 7 also shows that the linear relationship described by Eq. (20) does not apply for the case of superposed amine groups. On the other hand, using three principal

Table 7
Statistics for the four regression models based in Eq. (20)

	M1[a]	M2[a]	M3[a]	M4[a]	M1[b]	M2[b]	M3[b]	M4[b]
R^2	0.968	0.085	0.053	0.147	0.999	0.995	0.225	0.157
R.M.S.E.	0.014	0.039	0.076	0.037	0.004	0.004	0.098	0.052
Prob$>F$ (%)[c]	3.2	91.5	94.7	85.3	3.8	8.8	95.1	97.2
% Variance	78.4	79.5	78.7	92.7	99.2	99.5	98.3	97.6

[a] Two principal components used. Percentage of total variance recovered greater than 78%.
[b] Three principal components used. Percentage of total variance recovered greater than 97%.
[c] Obtained from $F_{3,1}$ and $F_{2,2}$ distributions for the three and two principal components cases, respectively.

The four cases correspond to overlap and Coulomb indices with superposed pyridinic rings (M1 and M2), and overlap and Coulomb indices with superposed amine groups (M3 and M4). The table collects the squared correlation coefficient (R^2), the root mean squared error (R.M.S.E.), the probability (%) of the null hypothesis (non-linear relationship) based on the F-test (Prob$>F$) and finally, the percent of the total variance recovered (% Variance) with the selected principal components.

components, a good linear relationship ($R^2 > 0.99$ and R.M.S.E. < 0.001) is found for the superposed pyridinic rings with both, overlap and Coulomb indices. It is interesting that, in the four cases, more than 78% of the variance is recovered using only two principal components, see Table 7. However, using two principal components, the linear relationship is only maintained for the case of overlap indices and superposed pyridinic rings.

The linear relationship found when pyridinic rings are superposed, and the lack of relationship for superposed amine groups, could reflect the form of the interaction with the receptor. These results are compatible with the hypothesis of a protonated pyridinic nitrogen playing and active role in the interaction process. This is again in agreement, as the previously discussed variation of interaction energy for the formation of the complex with the receptor, with the capacity of the protonated pyridinic nitrogen to act in a cation–π interaction or as a hydrogen donor in a hydrogen bond. Due to the four-fold symmetry of the pore in the K^+ channel and consequently, of the putative receptor sites [18], the amine groups of the different aminopyridines can be involved, in addition, in one or more hydrogen bonds with amino acid residues.

A good linear relationship is found for the overlap indices with two and three principal components when the rings are superposed. This result can be interpreted as expressing than the interaction is not due to pure electrostatic factors. However, the linear relationship found for the Coulomb indices with three principal components (but not with two) shows that electrostatic effects must play some role in the interactions. These results can be expected considering, again, that the blocking of the K^+ channel could involve a cation–π interaction, or a hydrogen bond formation with the additional hydrogen on the pyridinic ring. The linear relationship with the Coulomb indices can be attributed to the electrostatic component present in these two bonding forms [33,34].

5. Conclusions

In this work we develop a functional model of activity for the K^+ channel blocking by aminopyridines. We show that the logarithm of the experimental activity index (concentration of neutral form that produces a given result) depends linearly on the pK_a and the affinity (G) for the receptor.

Using the model, the order of affinity for the receptor is found different from the raw order of in vitro activity. The computed results for the affinity are compatible with previous data on the interaction energy of aminopyridines in cation–π complexes. These data suggest that the positive charge, a consequence of protonation, is not only used to permit the introduction of the charged aminopyridine into the pore of the K^+ channel. It seems, also, that the additional proton is actively and specifically involved in the binding to the receptor site. This can be achieved through a cation–π interaction or by formation of a donor hydrogen bond.

The quantum similarity theory is applied to the functional activity model. In this way, we found a linear relationship between a transformed activity index and the principal components of the similarity matrix. The model is validated with the experimental data. The fact that only five data points are available for statistical treatment forces us to be very careful in the interpretation of results. With this limitation, the results clearly support the proposed model, and the assumption of a ligand–receptor entropy variation as a function of the ligand. In addition, the present results show that not only the amine groups, but also the pyridinic ring must be actively involved in the interaction with the receptor site. Also, the results suggest, according to previous evidence, that a pure electrostatic interaction is not involved in the binding to the receptor site. The role of the amine groups in the interaction process can be the formation of one or more hydrogen bonds with the amino acid residues in the receptor site. Despite the different relative position of the amine groups respect to the pyridinic nitrogen, the C_4 symmetry of the inner part of the pore in the K^+ channel permits the formation of a multiple hydrogen bonded structure.

Acknowledgments

AN and CMC wish to thank the DGESIC (grant # PM98-0073) and the Universidad de Castilla-

La Mancha for financial support. XG acknowledges the University of Girona for a predoctoral fellowship. Fundació Mª Franscisca de Roviralta is also acknowledged.

References

[1] G.E. Kirsch, T. Narahashi, 3,4-Diaminopyridine. A potent new potassium channel blocker, Biophys. J. 22 (1978) 507–512.

[2] J. Molgó, M. Lemeignan, F. Peradejordi, P. Lechat, Effects présynaptiques des aminopyridines a la junction neuromusculaire de vertébrés, J. Pharmacol. (Paris) 16 (Suppl. II) (1985) 109–144.

[3] C. Carlsson, I. Rosen, E. Nilsson, Can 4-aminopyridine be used to reverse anaesthesia and muscle relaxation?, Acta Anaesthesiol. Scand. 27 (1993) 87–90.

[4] K.M. McEvoy, A.J. Windebank, N.J.R. Daube, P.A. Low, 3-4-Diaminopyridine in the treatment of Lambert–Eaton myasthenic syndrome, N. Engl. J. Med. 321 (1989) 1567–1571.

[5] S.R. Schwid, M.D. Petrie, M.P. McDermott, D.S. Tierney, D.H. Maso, A.D. Goodman, Quantitative assessment of sustained-release 4-aminopyridine for symptomatic treatment of multiple sclerosis, Neurology 48 (1997) 817–821.

[6] J.L. Segal, S.R. Brunnemann, 4-Aminopyridine improves pulmonary function in quadriplegic humans with longstanding spinal cord injury, Pharmacotherapy 17 (1997) 415–423.

[7] L.C. Sellin, The action of botulinum toxin at the neuromuscular junction, Med. Biol. 59 (1981) 11–20.

[8] M. Davidson, J.H. Zemishlany, R.C. Mohs, T.B. Horvath, P. Powchik, J.P. Blass, et al., 4-Aminopyridine in the treatment of Alzheimer's disease, Biol. Psychiatry 23 (1988) 485–490.

[9] I. Wickelgren, Animal studies raise hopes for spinal cord repair, Science 297 (2002) 178–181.

[10] J.I. Gillespie, O.F. Hutter, The actions of 4-aminopyridine on the delayed potassium current in skeletal muscle fibres, J. Physiol. (Lond.) 252 (1975) 70P–71P.

[11] J. Molgó, H. Lundh, S. Thesleff, Potency of 3, 4-diaminopyridine and 4-aminopyridine on mammalian neuromuscular transmission and the effect of pH changes, Eur. J. Pharmacol. 61 (1980) 25–34.

[12] G.E. Kirsch, T. Narahashi, Site of action and active form of aminopyridines in squid axon membranes, J. Pharmacol. Exp. Ther. 226 (1983) 174–179.

[13] J. Molgó, M. Lemeignan, P. Lechat, F. Peradejordi, Increase in evoked transmitter release from motor nerve terminals by some amino N-heterocyclic compounds, I, Eur. J. Med. Chem. 20 (1985) 149–153.

[14] J.R. Howe, J.M. Ritchie, On the active form of 4-aminopyridine:block of K^+ currents in rabbit Schwann cells, J. Physiol. 433 (1991) 183–205.

[15] D. Choquet, H. Korn, Mechanism of 4-aminopyridine action on voltage-gated potassium channels in lymphocytes, J. Gen. Physiol. 99 (1992) 217–240.

[16] F. Peradejordi, J. Molgó, M. Lemeignan, Increase in evoked transmitter release from motor nerve terminals by some amino N-heterocyclic compounds. II, Eur. J. Med. Chem. 20 (1985) 155–161.

[17] A. Niño, C. Muñoz-Caro, Theoretical analysis of the molecular determinants responsible for the K^+ channel blocking by aminopyridines, Biophys. Chem. 91 (2001) 49–60.

[18] C. Muñoz-Caro, A. Niño, The nature of the receptor site for the reversible K^+ channel blocking by aminopyridines, Biophys. Chem. 96 (2002) 1–14.

[19] R. Carbó-Dorca, D. Robert, L.I. Amat, X. Girones, E. Besalú, Molecular quantum similarity in QSAR and drug design, Lecture Notes in Chemistry, 73,, Springer-Verlag, 2000.

[20] J. Molgó, M. Lemeignan, P. Lechat, Effects of 4-aminopyridine at the frog neuromuscular junction, J. Pharmacol. Exp. Ther. 203 (1977) 653–663.

[21] K. Lucas, Applied Statistical Thermodynamics, Springer-Verlag, 1991.

[22] R. Carbó, E. Besalú, L.I. Amat, X. Fradera, Quantum molecular similarity measures (QMSM) as a natural way leading towards a theoretical foundation of quantitative structure–properties relationships (QSPR), J. Math. Chem. 18 (1995) 237–246.

[23] R. Carbó-Dorca, E. Besalú, Quantum theory of QSAR, Contributions to Science, 1, Institut d'Estudis Catalans, Barcelona, 2000, pp. 399–422.

[24] R. Bonaccorsi, E. Scrocco, J. Tomasi, Molecular SCF calculations for the ground state of some three-members ring molecules: $(CH_2)_3$, $(CH_2)_2NH$, $(CH_2)_2NH_2^+$, $(CH_2)_2O$, $(CH_2)_2S$ $(CH)_2CH_2$ and N_2CH_2, J. Chem. Phys. 52 (1970) 5270–5284.

[25] R. Carbó-Dorca, E. Besalú, Fundamental quantum QSAR (Q^2SAR) equation: extensions, nonlinear terms and generalizations within extended Hilbert–Sobolev spaces, Int. J. Quantum Chem. 88 (2002) 167–182.

[26] R. Ponec, L. Amat, R. Carbó-Dorca, Quantum similarity approach to LFER: substituent and solvent effects on the acidities of carboxylic acids, J. Phys. Org. Chem. 12 (1999) 447–454.

[27] R. Carbó, L. Leyda, M. Arnau, How similar is a molecule to another? An electron density measure of similarity between two electronic structures, Int. J. Quantum Chem. 17 (1980) 1185–1189.

[28] R.A. Johnson, D.W. Wichern, Applied Multivariate Analysis, 5th, Prentice-Hall, 2002.

[29] L. Amat, R. Carbó-Dorca, Quantum similarity measures under atomic shell approximation: first order density fitting using elementary Jacobi rotations, J. Comput. Chem. 18 (1997) 2023–2039.

[30] X. Gironés, R. Robert, R. Carbó-Dorca, TGSA: a molecular superposition program based on topo-geometrical considerations, J. Comput. Chem. 22 (2001) 255–263.

[31] Small Stata for Windows 98/95/NT, Stata Corporation, 2000.
[32] M.J.S. Dewar, A Semiempirical Life, American Chemical Society, 1992, pp. 160–162.
[33] M.D. Ryan, Chapter 4. Effect of hydrogen bonding on molecular electrostatic potential, in: D.A. Smith (Ed.), Modeling the Hydrogen Bond, ACS Symposium series 569, American Chemical Society, 1994.
[34] J.C. Ma, D.A. Dougherty, The cation–π interaction, Chem. Rev 97 (1997) 1303–1324.